

Polymer Neural Interface with Dual-Sided Electrodes for Neural Stimulation and Recording

Angela Tooker, Vanessa Tolosa, Kedar G. Shah, Heeral Sheth, Sarah Felix, Terri Delima, Satinderpall Pannu

Abstract— We present here a demonstration of a dual-sided, 4-layer metal, polyimide-based electrode array suitable for neural stimulation and recording. The fabrication process outlined here utilizes simple polymer and metal deposition and etching steps, with no potentially harmful backside etches or long exposures to extremely toxic chemicals. These polyimide-based electrode arrays have been tested to ensure they are fully biocompatible and suitable for long-term implantation; their flexibility minimizes the injury and glial scarring that can occur at the implantation site. The creation of dual-side electrode arrays with more than two layers of trace metal enables the fabrication of neural probes with more electrodes without a significant increase in probe size. This allows for more stimulation/recording sites without inducing additional injury and glial scarring.

I. INTRODUCTION

Micro-electrode neural interfaces are an essential tool in neuroscience. By targeting neuronal activity, neural interfaces enable researchers and clinicians to better explore and understand neurological processes and diseases. Moreover, such devices can be used to bypass damaged tissue and stimulate or record neural activity, thereby restoring lost communication and/or control with the affected parts of the nervous system.

The most common neural interfaces are thin-film micro-machined probes fabricated on silicon substrates using MEMS fabrication techniques [1-4]. Neuronal stimulation and recording is conducted at discrete sites (electrodes) along the probes. The electrodes are connected, via metal traces, to output leads or other signal processing circuitry. Silicon is the most widely used substrate for this type of probe because of its many unique physical/electrical characteristics. Further, the prevalence of silicon in the microelectronics industry ensures the neural interfaces can be easily and efficiently fabricated in large numbers utilizing common MEMS fabrication techniques. There are, however, significant concerns regarding the suitability of these silicon-based neural interfaces for long-term (i.e. chronic) *in vivo* studies [5]. In addition, the continuous micro-motion of the neural tissue can induce strain between the neural tissue and

implanted neural interface inducing chronic injury and glial scarring at the implant site. These outstanding questions regarding the long-term safety and functionality of these silicon-based neural interfaces have prompted the development of polymer-based interfaces.

Polymer-based neural interfaces are an attractive alternative to traditional silicon-based interfaces. First, they are flexible, thereby minimizing the strain between the neural tissue and the implanted probe [6]. Second, they are fully biocompatible, if fabricated properly, and thus suitable for chronic implantation with no loss of functionality or safety [7]. Finally, these polymer-based neural interfaces can be easily fabricated in large numbers using existing MEMS fabrication techniques. Various polymer-based neural interfaces have been fabricated using either polyimide or parylene [8-15] and have proven to be successful for intra-neural stimulation and recording in both cochlear and retinal implants.

Although the flexibility of the polymer-based neural interfaces minimizes the strain induced on the neural tissue when implanted, it does not eliminate it. Thus, some injury and glial scarring occurs at the implant site. There are two primary means for minimizing the degree of injury and scarring: 1) utilizing materials with mechanical properties similar to that of neural tissue and 2) minimizing the size of the implanted probe. Flexible polymers, like polyimide and parylene, have mechanical properties more closely matched to that of neural tissue, compared to silicon, which minimizes injury. Unfortunately, minimizing the size of the implanted probe limits the number of stimulation/recording sites (electrodes) that can be fabricated on a single probe. This, in turn, limits the number of neurons that can interface with a single probe. Neural interfaces with electrodes on two sides (as opposed to the standard one side) have twice the number of stimulation/recording sites without creating a significant increase in probe size or decreasing the inter-electrode spacing. The typical problem encountered when creating dual-sided neural interfaces, however, is how to easily and efficiently fabricate them using common MEMS fabrication techniques.

Several processes have been developed for creating polymer-based, dual-side neural interfaces [13-15]. Stieglitz et al. build the neural interfaces from the bottom up: bottom polyimide layers, electrodes and interconnection traces, followed by the top interconnection traces, electrodes and polyimide layers [13]. The difficulty in this fabrication process is with the opening of the bottom electrodes. The top electrodes, being on the “top” during fabrication, are simply etched open. Unfortunately, the bottom electrodes

*Research supported by National Institute of Deafness and Other Communication Diseases.

A. C. Tooker is with Lawrence Livermore National Laboratory, Livermore, CA 94550 USA (phone: 925-422-2326; fax: 925-422-2373; e-mail: tooker1@llnl.gov).

V. Tolosa, K.G. Shah, H. Sheth, S. Felix, T. Delima, and S. Pannu are with Lawrence Livermore National Laboratory, Center for Micro- and Nano-Technology, Livermore, CA 94550 USA (e-mail: tolosa1@llnl.gov, shah22@llnl.gov, sheth2@llnl.gov, felix5@llnl.gov, delima1@llnl.gov, pannu1@llnl.gov).

are not exposed during the fabrication. In the method described by Stieglitz et al., the entire polyimide film on the wafer is released and then turned over, thereby placing the bottom electrodes on “top.” The bottom electrodes are then etched open. This final step of releasing the polyimide film can be extremely problematic and requires very careful handling and preparation of the polymer film to ensure proper, uniform, and reproducible etching when opening the bottom electrodes.

Doerge et al. [14] have developed a process that minimizes some of the complexity inherent in Stieglitz’s process. The fabrication process is identical to that described by Stieglitz until the final step of opening the bottom electrodes is reached. Instead of removing the polyimide film and then etching the bottom electrodes open, in the process described by Doerge et al., the backside of the wafer is etched at the locations of the bottom electrodes. The bottom electrodes are then etched open, without the need for removing the thin polyimide film from the wafer. Although this process demonstrates an improvement from that described in the previous paper, there are still several significant drawbacks with this process. First, the chemical used during the backside bulk etch step (potassium hydroxide) is harmful to the polyimide used in fabricating the neural interface. Although steps are taken to minimize the polyimide’s exposure, the long etching time required for the backside etch is a significant cause for concern for the yield and efficacy of the probes. In addition, this process requires additional protective materials (i.e. silicon nitride) to be deposited and subsequently removed, further increasing the overall complexity of the process.

Recently, Seymour et al. demonstrated another technique for creating flexible, parylene-based dual-sided neural interface [15]. This technique utilizes a layer of SiO₂ as both a release layer and an electrode place holder. Unfortunately, this process requires both chemical mechanical polishing of the parylene as well as very long (multi-hour) soaks in hydrofluoric acid (HF). Although the use of chemical mechanical polishing does increase the complexity of the fabrication process, of greater concern is the long HF soak required to release the probe from the substrate. It has been demonstrated that HF easily penetrates through parylene, even after only 10 minutes of exposure [16]. This poses the question of how much HF remains in the probe after fabrication and, due to the extremely toxic nature of HF, whether the neural interfaces are safe for chronic, long-term implantation.

Dual-side neural interfaces, such as the thin-film LIFE system, have also been developed for use in the peripheral nervous system [17-18]. However, these interfaces typically have a very large footprint and are not well-suited for the central nervous system.

We present a polyimide-based, dual-side, micro-electrode neural interface suitable for neural stimulation and recording. Unlike previously presented dual-side neural probes, the fabrication process utilized here does not require: 1) removal/re-attachment of the polyimide film, 2) long and potentially-harmful backside etches, 3) chemical mechanical polishing, or 4) multi-hour exposure to hydrofluoric acid.

The device footprints are also small enough for use in the central nervous system. In addition, this micro-electrode probe is comprised of 4 layers of trace metal, as opposed to the 1 or 2 utilized in other neural interface fabrication [8-16] (dual-sided or single-sided). This further increases the number of individually-addressable electrode stimulation/recording sites on the neural interface without a significant increase in probe size.

II. NEURAL INTERFACE DESIGN AND FABRICATION

Several different neural interfaces were designed and fabricated with electrode diameters ranging from 10 μm to 100 μm in both linear and tetropde spatial orientations. All of the electrodes are individually addressable. Each electrode side (top and bottom) utilizes two layers of trace metal. The layers of trace metal are connected using interconnection vias.

The general fabrication process is summarized in Fig. 1. The fabrication begins with a standard silicon wafer that is then etched with SF₆ plasma to create silicon posts at the bottom electrode sites (Fig. 1A). A sacrificial release layer (typically chrome) is evaporated onto the silicon wafer. A single layer of polyimide is then deposited to planarize the surface (Fig. 1B). The use of the silicon posts creates an electrode that is recessed from the bottom polyimide surface. This generates a more uniform electric field, compared to that generated by an electrode flush with the polyimide surface [19].

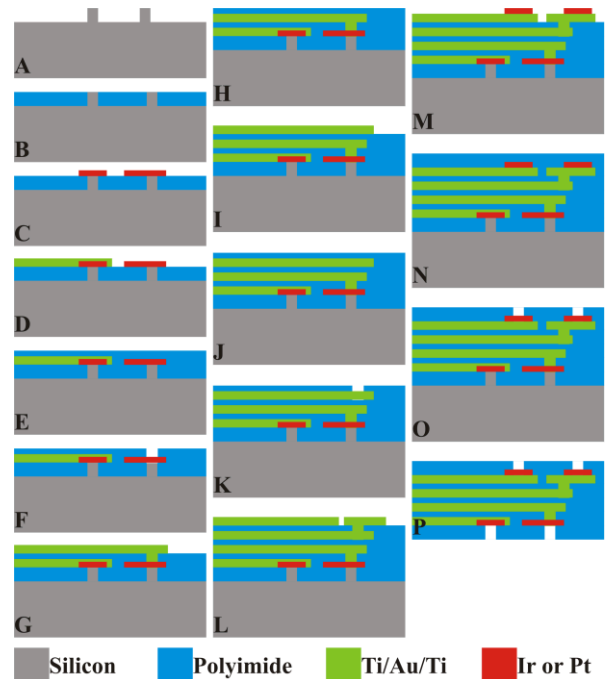


Figure 1. Cross-sectional view of the general fabrication process presented here for the dual-side, 4-layer trace metal, polymer neural interface. This is a single-side process requiring only simple polymer/metal deposition and etching steps. (Images are not drawn to scale.)

Next, the bottom electrode metal, either iridium or platinum, is deposited and patterned (Fig. 1C). The first layer of trace metal (Ti/Au/Ti) is deposited/patterned and the interlayer of polyimide is then deposited (Figs. 1D-1E).

Interconnection vias are etched through the polyimide with O_2 plasma (Fig. 1F). The second, third, and fourth layers of trace metal are next deposited and patterned, with additional layers of polyimide and interconnection vias between each trace metal layer (Figs. 1G-1L).

After the fourth layer of trace metal, the top electrode metal, either iridium or platinum, is deposited and patterned (Fig. 1M). The final polyimide layer is deposited (Fig. 1N) and the top electrode vias and device outlines are then etched with O_2 plasma (Fig. 1O). Finally, the devices are released from the wafer utilizing a wet chrome etchant (< 1 hour) (Fig. 1P).

We have demonstrated this process using polyimide. The same fabrication process can be used with other polymers, such as parylene and silicones. In the probes shown here, the topside and bottom-side electrodes are offset. The same fabrication process has been used to fabricate probes where the topside and bottom-side electrodes overlap. All of the electrodes, however, are individually addressable.

Photographs of three 4-layer metal, dual-side neural interfaces are shown in Figs. 2-5. (The interference patterns visible in Figs. 2-5 result from the non-uniformity of the polyimide laying down on the glass slide.) The dual-side probe shown in Fig. 2 has variable sized electrodes with electrode diameters ranging from $10\ \mu\text{m}$ to $100\ \mu\text{m}$. The dual-side probe in Fig. 3 has $20\ \mu\text{m}$ diameter electrodes in a tetrode arrangement. For both of these probes, the electrodes are in groups of four and these groups alternate between top and bottom electrodes, with the topside electrodes closest to the probe tip. Fig. 4 shows a dual-side, 4-layer metal probe with constant $100\ \mu\text{m}$ diameter electrodes. The electrodes alternate between topside and bottom-side electrodes. An enlarged view of the topside and bottom-side electrodes is shown in Fig. 5.

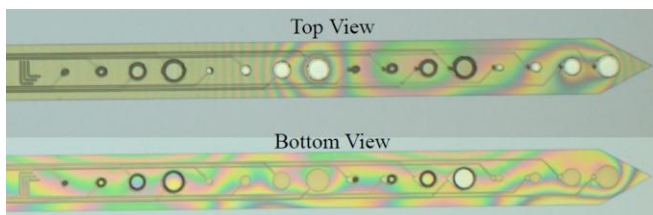


Figure 2. A dual-side, 4-layer metal, neural interface with variable sized electrodes. The electrode diameters are: $10\ \mu\text{m}$, $30\ \mu\text{m}$, $70\ \mu\text{m}$, and $100\ \mu\text{m}$. A top view and bottom view are shown. From left to right, the first 4 electrodes are bottom-side, followed by 4 topside electrodes, followed by 4 bottom-side, and finally 4 more topside electrodes at the probe tip.

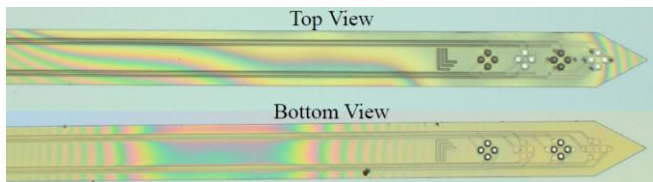


Figure 3. A dual-side, 4-layer metal, neural interface with $20\ \mu\text{m}$ diameter electrodes. A top view and bottom view are shown. The tetrodes alternate between bottom-side and topside electrodes (the electrodes closest to the probe tip are topside).

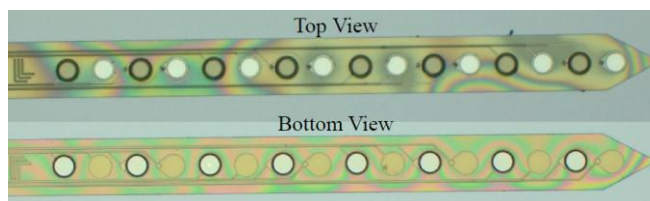


Figure 4. A dual-side, 4-layer metal, neural interface with $100\ \mu\text{m}$ diameter electrodes. A top view and bottom view are shown. The electrodes alternate between bottom-side and topside (the electrodes closest to the probe tip are topside).

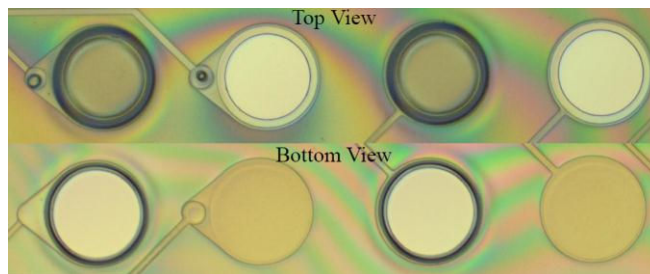


Figure 5. An enlarged view of the $100\ \mu\text{m}$ diameter electrodes is shown here. The electrodes alternate between bottom-side and topside (the left-most electrodes are bottom-side).

III. NEURAL INTERFACE ELECTRODE CHARACTERIZATION

A. Electrochemical Testing

The iridium activation was performed using biphasic potential pulsing in phosphate-buffered saline to form an activated iridium oxide film (AIROF). Individual iridium electrodes were characterized to determine charge storage capacity (CSC) and impedance both before and after activation. Cyclic voltammetry (CV) and electrochemical impedance measurements were made with a Princeton Applied Research (PAR) potentiostat using vendor-supplied software. All measurements were made in a three-electrode cell using a Pt counter electrode, an Ag/AgCl reference electrode, and phosphate-buffered saline (pH 7.4) as the electrolyte. Potential cycling for the CVs was performed between $-600\ \text{mV}$ and $+800\ \text{mV}$ at a scan rate of $100\ \text{mV/s}$.

A typical CV curve of one of the bottom-side $100\ \mu\text{m}$ electrodes is shown in Fig. 6. As can be seen, the characteristic iridium oxide peaks are clearly visible after activation. The CSC of the AIROF for the topside electrodes ($100\ \mu\text{m}$ diameter) is $21.8\ \text{mC/cm}^2$ and for the bottom-side electrodes ($100\ \mu\text{m}$ diameter) is $14.0\ \text{mC/cm}^2$. The impedance (at $f = 1\ \text{kHz}$) for the AIROF topside electrodes is $3.3\ \text{k}\Omega$ and for the AIROF bottom-side electrodes is $3.8\ \text{k}\Omega$. CV curves and electrode impedances ideally overlap for a given electrode geometry. The impedances for the topside and bottom-side electrodes exhibit no significant variation. The cause of the differences in the CSCs is currently being investigated. The other electrode sizes exhibit similar results.

B. Biocompatibility Testing

The selection and evaluation of materials and devices intended for use in humans requires a structured program of assessment to establish biocompatibility and safety. In order

to qualify our devices for chronic implantation in accordance with the FDA regulations, we have subjected our single-sided platinum neural interfaces to the ISO-10993 array of biocompatibility testing for chronically implanted devices. This includes assessing the biological reactivity, allergenic potential, sensitizing capacity, systemic toxic effects, immune response, and genetic mutations in animal models that are exposed to the device. The single-sided iridium neural interfaces have not been subjected to the complete array of testing, but they have successfully passed basic cytotoxicity screening. We expect the dual-sided neural interfaces presented here to also successfully pass biocompatibility testing, due to the inherent similarities in material selection and fabrication processes to previously tested devices.

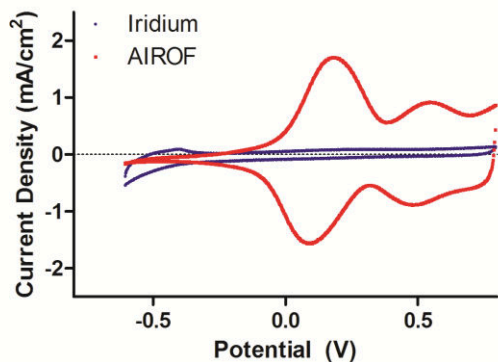


Figure 6. Typical CV curve of a bottom-side 100 μm diameter AIROF electrode before and after electrochemical activation. After activation, the characteristic iridium oxide peaks are clearly visible. Although the CV curves do not completely overlap, both the topside and bottom-side AIROF electrodes exhibit these same characteristic peaks.

IV. CONCLUSION

We have presented here a new and more efficient method for creating polymer-based, dual-side, micro-electrode neural interfaces utilizing 4 layers of trace metal to achieve a higher electrode count for given probe dimensions. These probes are currently undergoing further lifetime (both electrode and probe) testing. Preliminary long-term *in vivo* testing of similarly fabricated, single-sided neural interfaces have demonstrated neural recording capabilities more than 50 days, post-implantation. Long-term *in vivo* testing of these dual-sided neural interfaces is underway.

ACKNOWLEDGMENT

This work has been funded by the National Institute of Deafness and Other Communication Diseases. This work performed under the auspices of the U.S. Department of Energy by Lawrence Livermore National Laboratory under Contract DE-AC52-07NA27344. LLNL-ABS-538812.

REFERENCES

[1] A. Sharma, L. Rieth, P. Tathireddy, R. Harrison, H. Oppermann, M. Klein, M. Topper, E. Jung, R. Normann, G. Clark, and F. Solzbacher, "Long term *in vitro* functional stability and recording longevity of fully integrated wireless neural interfaces based on the Utah Slant Electrode Array," *J. Neural. Eng.*, vol. 8, no. 4, August 2011.

[2] C. Chestek, V. Gilja, P. Nuyujukian, J. Foster, J. Fan, M. Kaufman, M. Churchland, Z. Rivera-Alvidrez, J. Cunningham, S. Ryu, and K. Shenoy, "Long-term stability of neural prosthetic control signals from silicon cortical arrays in rhesus macaque motor cortex," *J. Neural Eng.*, vol. 8, no. 4, August 2011.

[3] D. Fan, D. Rich, T. Holtzman, P. Ruther, J. Dalley, A. Lopez, M. Rossi, J. Barter, D. Salas-Meza, S. Herwik, T. Holzhammer, J. Morizio, and H. Yin, "A Wireless Multi-Channel Recording System for Freely Behaving Mice and Rats," *PLoS ONE*, vol. 6, no. 7, 2011.

[4] M. Azin, D. Guggenmos, S. Barbay, R. Nudo, and P. Mohseni, "A Miniaturized System for Spike-Triggered Intracortical Microstimulation in an Ambulatory Rat," *IEEE Trans. Biomed. Eng.*, vol. 58, no. 9, pp. 2589-2597, September 2011.

[5] R. Biran, D. Martin, and P. Tresco, "Neuronal cell loss accompanies the brain tissue response to chronically implanted silicon microelectrode arrays," *Exp. Neurology*, vol. 195, pp. 115-126, 2005.

[6] V. Polikov, P. Tresco, and W. Reichert, "Response of brain tissue to chronically implanted neural electrodes," *J. Neurosci. Meth.*, vol. 148, pp. 1-18, 2005.

[7] Y. Sun, S. Lacour, R. Brooks, R. Rushton, J. Fawcett, and R. Cameron, "Assessment of the biocompatibility of photosensitive polyimide for implantable medical device use," *J. Biomed. Mat. Res. A*, vol. 90A, no. 3, pp. 648-655, September 2009.

[8] W. Tsang, A. Stone, Z. Aldworth, J. Hildebrand, T. Daniel, A. Akinwande, and J. Voldman, "Flexible Split-Ring Electrode for Insect Flight Biasing Using Multisite Neural Stimulation," *IEEE Trans. Biomed. Eng.*, vol. 57, no. 7, pp. 1757-1764, July 2010.

[9] S. Lee, J. Jung, Y. Chae, J.-K. Suh, and J. Kang, "Fabrication and characterization of implantable flexible nerve cuff electrodes with Pt., Ir, and IrO_x films deposited by RF sputtering," *J. Micromech. Microeng.*, vol. 20, no. 3, March 2010.

[10] B. Rubehn, C. Bosman, R. Oostenveld, P. Fries, and T. Stieglitz, "A MEMS-based flexible multi-channel ECoG-electrode array," *J. Neural Eng.*, vol. 6, no. 3, June 2009.

[11] A. Mercanzini, K. Cheung, D. Buhl, M. Boers, A. Maillard, P. Colin, J.-C. Bensadoun, A. Bertsch, and P. Renaud, "Demonstration of cortical recording using novel flexible polymer neural probes," *Sens. Actuators A*, vol. 143, pp. 90-96, 2008.

[12] K. Cheung, P. Renaud, H. Tanila, and K. Djupsund, "Flexible polyimide microelectrode array for *in vivo* recordings and current source density analysis," *Biosens. Bioelectron.*, vol. 22, pp. 1783-1790, 2007.

[13] T. Stieglitz, "Flexible biomedical microdevices with double-sided electrode arrangements for neural applications," *Sens. Actuators A*, vol. 90, pp. 203-211, 2001.

[14] T. Doerge, S. Kammer, M. Hanauer, A. Sossalla, S. Steltenkamp, "Novel method for a flexible double sided microelectrode fabrication process," *Bioengineered and Bioinspired Systems IV Book Series: Proc. Of SPIE*, vol. 7365, 2009.

[15] J. Seymour, N. Langhals, D. Anderson, and D. Kipke, "Novel multi-side, microelectrode arrays for implantable neural applications," *Biomed. Microdevices*, vol. 13, pp. 441-451, February 2011.

[16] M. Liger, D. Rodger, and Y.C. Tai, "Robust Parylene-to-Silicon Mechanical Anchoring," in *Proc. 16th Annu. IEEE Int. Conf. Micro Electro Mech. Sys. (MEMS '03)*, Kyoto, Japan, January 2003, pp. 602-605.

[17] P. Rossini, S. Micera, A. Benvenuto, J. Carpaneto, G. Cavallo, L. Citi, C. Cipriani, L. Denaro, V. Denaro, G. Di Pino, F. Ferreri, E. Guglielmelli, K.-P. Hoffman, St. Raspopovic, J. Rigosa, L. Rossini, M. Tombini, and P. Dario, "Double nerve intraneural interface implant on a human amputee for robotic hand control," *Clinical Neurophys.*, vol. 121, pp. 777-783, 2010.

[18] L. Citi, J. Carpaneto, K. Yoshida, K.-P. Hoffmann, K.P. Koch, P. Dario, and S. Micera, "On the use of wavelet denoising and spike sorting techniques to process electroneurographic signals recorded using intraneural electrodes," *J. Neurosci. Meth.*, vol. 172, pp. 294-302, 2008.

[19] M. Suesserman, F. Spelman, and J. Rubinstein, "In Vitro Measurement and Characterization of Current Density Profiles Produced by Nonrecessed, Simple Recessed, and Radially Varying Recessed Stimulating Electrodes," *IEEE Trans. Biomed. Eng.*, vol. 38, no. 5, pp. 401-408, 1991.